



Cite this: *Org. Biomol. Chem.*, 2024, **22**, 8781

Lighting up *Mycobacteria* with membrane-targeting peptides†

Zainab S. Alghamdi,^{†a,b} Richa Sharma,^{†a} Nancy Kiruthiga,^c Muhammed Üçüncü,^{†a,d} Maxime Klausen,^a Mithun Santra,^{†a} Uma Devi,^c Seshasailam Venkateswaran,^e Annamaria Lilienkampf^{†a} and Mark Bradley^{†a,e}

Received 11th August 2024,
Accepted 6th October 2024

DOI: 10.1039/d4ob01333f

rsc.li/obc

We report a series of fluorescent probes based on mycobacteria membrane-associated disruption peptide, containing either L- or D-amino acids which were originally designed to kill *Mycobacterium tuberculosis* via membrane disruption. These peptides were decorated with “always on” and environmentally sensitive fluorophores and showed the rapid and efficient labelling of *Mycobacterium smegmatis*, with labelling of *Mycobacterium tuberculosis* demonstrated by two of the probes.

Introduction

Tuberculosis (TB) affects an estimated one-fourth of the world's population and remains a prominent cause of death with its high infectiousness and mortality.¹ The COVID-19 pandemic has had huge detrimental consequences by hampering access to TB diagnosis and treatment, as well as increasing its prevalence due to “lock-downs” promoting transmission.² Indeed, much of the rapid progress made in the five years prior to 2020 has been undone, many people undiagnosed/untreated during the pandemic, with an additional 10.6 million people diagnosed in 2021, and with 2–3 times as many deaths from TB every decade than from COVID-19 to date.^{3,4}

A key need for a successful TB treatment campaign is early diagnosis, to prevent the spread of infection and permitting early therapeutic intervention. Diagnosis still mainly relies on the direct detection of *Mycobacterium tuberculosis* (*Mtb*), the causative pathogen of TB, by a traditional smear analysis and staining, although microbial culture and genetic methods are

becoming more mainstream.^{1,2} Smear sputum microscopy relies on acid-fast staining of *Mtb* in sputum, using the Ziehl-Neelsen (colour-based) or auramine–rhodamine (fluorescence-based) staining.^{5,6} However, key drawbacks of sputum smears are their lack of sensitivity and specificity. Indeed, factors such as sample collection and preparation can drastically affect the outcomes and sensitivity of Ziehl-Neelsen staining.^{7,8} Auramine–rhodamine staining provides high sensitivity but there is a lack of selectivity against other bacteria resulting in false positives. As such, there is a need to develop stains that are able to selectively and sensitively detect *Mtb*, allowing rapid, convenient and accurate early-stage identification of *Mtb* through sputum smear microscopy. Fluorescent probes are key entities for the detection of a range of microbial infections and cover several mechanistic classes.^{9–12} Activation of fluorogenic probes by specific bacterial enzymes, such as aminopeptidases and sulfatases are well known,^{13,14} while probes based on fluorescently labelled antibiotics have also been reported.¹⁵ Fluorophore-labelled trehalose has been reported to be metabolically incorporated into the mycobacterial cell envelope at high probe concentrations (100 μ M for *Mtb*),^{16–23} although labelling of autoclaved (dead) *Mycobacterium* has been found with some trehalose probes.²⁴

Natural host defence peptides have gained attention as potential antimicrobial therapeutics, and they often act *via* membrane-specific, bactericidal mechanisms that are capable of remarkably selective actions, making them distinct from traditional antibiotics.^{25,26} Although natural host defence peptides offer a pool of molecules, rational *de novo* design has also given peptides possessing novel bioactivity. In this regard, Medina reported a biomimetic, α -helical “defence peptide” (KRWHWRRHWVW-NH₂), referred to as a mycobacteria membrane-associated disruption peptide (MAD1), which was inspired by the unique features of the mycobacteria-specific

^aSchool of Chemistry, University of Edinburgh, David Brewster Road, EH9 3FJ Edinburgh, UK

^bDepartment of Chemistry, College of Science, Imam Abdulrahman Bin Faisal University, P. O. Box 1982, Dammam 31441, Saudi Arabia

^cIndian Council of Medical Research (ICMR) – National Institute for Research in Tuberculosis, No. 1, Mayor Sathiyamoorthy Road, Chetpet, Chennai – 600 031, India

^dDepartment of Analytical Chemistry, Faculty of Pharmacy, İzmir Katip Çelebi University, İzmir, Turkey

^ePrecision Healthcare University Research Institute, Queen Mary University of London, Empire House, Whitechapel, London, E1 1HH, UK.

E-mail: m.bradley@qmul.ac.uk

†Electronic supplementary information (ESI) available: Supporting figures and experimental procedures. See DOI: <https://doi.org/10.1039/d4ob01333f>

‡These authors contributed equally to the work.



transmembrane protein porin A that differs from porins of non-mycobacterial microbes.^{27,28} The peptide MAD1 was designed and optimised *in silico* to self-assemble within the mycolic-acid rich outer membrane of *Mtb*, with MAD1 found to selectively kill *Mtb* with an MIC of 2.5–5 μ M by induction of membrane defects, without notable activity against mammalian cells.^{29,30}

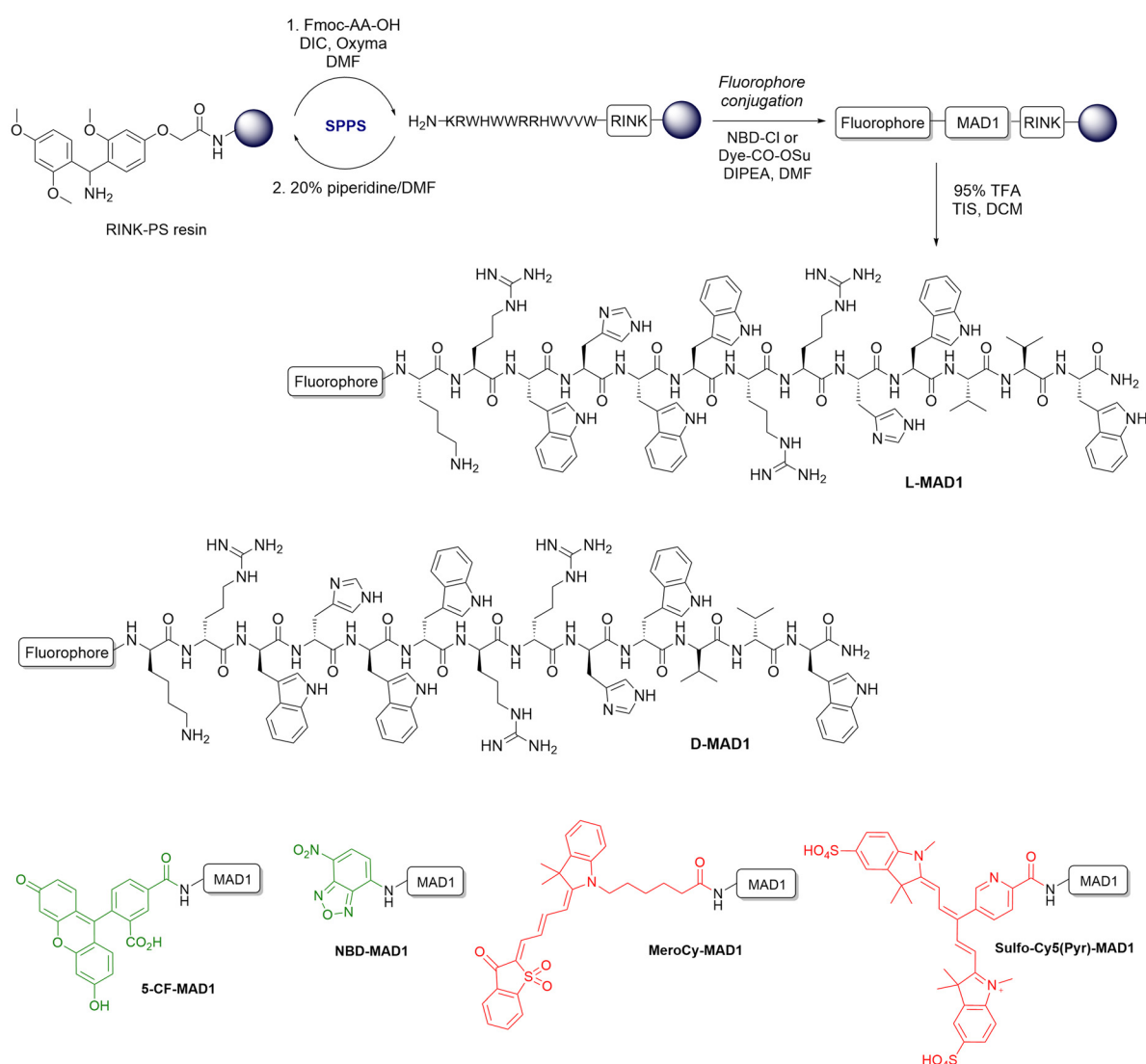
Here, we report a series of MAD1-based fluorescent probes (emission from 450 nm to 700 nm) and their evaluation against mycobacteria, including *Mtb*, based on both solvato-fluorogenic dyes nitrobenzoxadiazole (NBD, green) and merocyanine (MeroCy, orange)³¹ as well as more traditional “always-on” 5-carboxyfluorescein (5-CF, green)³² and sulfonated Cy5 (Sulfo-Cy5 (Pyr), red) fluorophores. The specific Cy dye (Sulfo-Cy5(Pyr)) was

chosen here due to its water solubility, convenient synthesis³³ and demonstrated success in biological labelling.³⁴ All the probes were synthesised *via* solid-phase methods and tested against *Mycobacterium smegmatis* (*M. smegmatis*) and *H37Rv*, a laboratory strain of *Mtb*, as well as clinically relevant strains of Gram-negative and Gram-positive bacteria.

Results and discussion

Probe design and syntheses

The rationally designed MAD1 peptides were reported to allow the specific targeting and killing of mycobacteria and, since our aim was the selective recognition and fluorescent labelling



Scheme 1 Design and synthesis of the MAD1-based fluorescent probes. The MAD1 peptide was synthesised on an Fmoc-Rink-linker functionalised polystyrene resin (loading 0.745 mmol g^{−1}, 100–200 mesh) using Fmoc-protected amino acids with Oxyma/DIC as the coupling combination. Upon synthesis of the MAD1 sequence, the fluorophores were coupled to the N-terminus using their respective NHS-esters, except for NBD where SNAr chemistry of NBD-Cl was used. After deprotection and resin cleavage, the peptides were purified by preparative HPLC and characterised by HRMS and HPLC (ESI Fig. S7–S16†).



of *Mtb*, the MAD1 peptide was identified as a suitable targeting ligand.²⁷ Four fluorophores were utilised for conjugation to the N-terminus of the peptide, to cover the wavelength range from green to NIR-I,^{35,36} with the environmentally sensitive fluorophores, NBD and MeroCy (which only become fluorescent in hydrophobic environments, here upon the interaction with the bacterial membrane) allowing “wash-free” labelling. In addition, both “L”- and “D”-enantiomers of MAD1 were investigated, as D-amino acid containing peptides are known to be robust to proteolysis.^{10,37} The probes were synthesised on solid-phase as shown in Scheme 1 (also see ESI Fig. S7–S16†).

Photophysical characterisation

The photophysical properties were determined for the probes (Table 1 and ESI Fig. S17, S18†), with the “always-on” MAD1 conjugates investigated in aqueous solution, while the environ-

mental MAD1 conjugates were investigated in more hydrophobic environments to mimic their emissive behaviour in bacterial membranes. For **NBD-L-MAD1** and **MeroCy-L-MAD1**, strong fluorescence emission was observed in DMSO, with the addition of water leading to a reduction in fluorescence (ESI Fig. S18†) mirroring the photophysical properties of the parent fluorophores.^{11,36} Circular dichroism spectroscopy showed that the addition of fluorophores to the N-terminus of the MAD1 peptide did not affect its helical secondary structure (at 206–219 nm), nor the exciton band observed at 228 nm (ESI Fig. S19†).

Bacterial labelling

Mycobacterial labelling was initially investigated with the non-infectious and fast-growing species *M. smegmatis* by confocal microscopy, with all eight probes (1–10 μM) showing rapid

Table 1 Photophysical properties of the “always-on” **5-CF-L-MAD1** and **Sulfo-Cy5(Pyr)-L-MAD1** and the “environmentally sensitive” **NBD-L-MAD1** and **MeroCy-L-MAD1** probes. For NBD and MeroCy, DMSO was used as a more hydrophobic environment to promote the probes’ maximal fluorescence

Compound	Solvent	$\lambda_{\text{abs}}^{\text{max}}$ (nm)	ϵ^{max} ($\text{M}^{-1} \text{cm}^{-1}$)	$\lambda_{\text{em}}^{\text{max}}$ (nm)	Stokes shift (cm^{-1})	Φ_{f}^a	$\epsilon^{\text{max}}\Phi_{\text{f}}$ ($\text{M}^{-1} \text{cm}^{-1}$)
5-CF-L-MAD1	H ₂ O/DMSO (9/1, v/v)	494	5.9×10^4	522	1086	0.17 ^a	10.0×10^3
Sulfo-Cy5(Pyr)-L-MAD1	H ₂ O/DMSO (9/1, v/v)	641	4.3×10^4	659	677	0.08 ^c	3.44×10^3
NBD-L-MAD1	DMSO	464	1.2×10^4	545	3203	0.06 ^a	0.72×10^3
MeroCy-L-MAD1	DMSO	600	2.4×10^4	627	717	0.02 ^b	0.48×10^3

Fluorescence quantum yield, derived from relative measurements using standards selected based on the absorption and emission properties of the probes. ^a Fluorescein in 0.1 M NaOH ($\Phi_{\text{f}} = 0.90$). ^b Rhodamine 6G in EtOH ($\Phi_{\text{f}} = 0.94$). ^c Cresyl violet in MeOH ($\Phi_{\text{f}} = 0.54$).

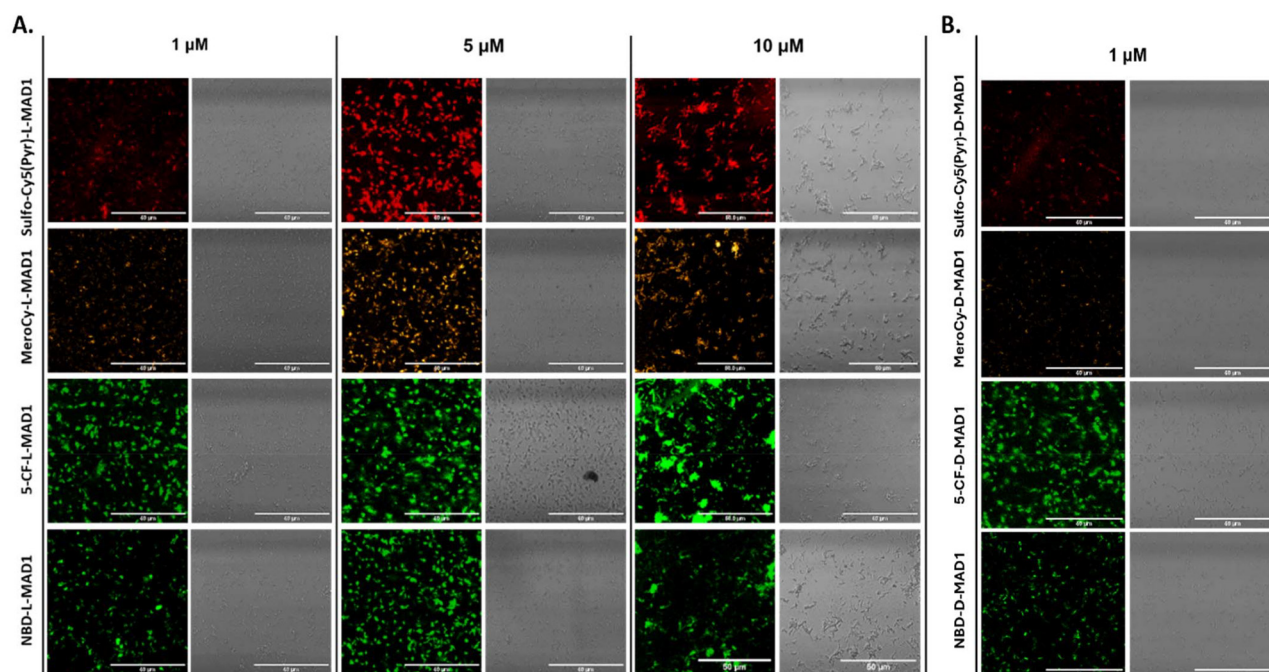


Fig. 1 (A) Concentration-dependent labelling of *M. smegmatis* with the L-MAD1-based probes. The bacteria were incubated with the probes (1, 5 or 10 μM) for 1 h, washed and imaged. Filters used for laser scanning confocal microscopy imaging (left panels): Cy5 for **Sulfo-Cy5(Pyr)-MAD1**, Alexa 594 for **MeroCy-L-MAD1**, Alexa 488 for **5-CF-L-MAD1** and **NBD-L-MAD1**. Panels right of all the fluorescent images are the brightfield images. (B) Comparison of the labelling of *M. smegmatis* with the “L” and “D” enantiomers of MAD1 probes (1 μM for 1 h). Scale bar = 50 μm .



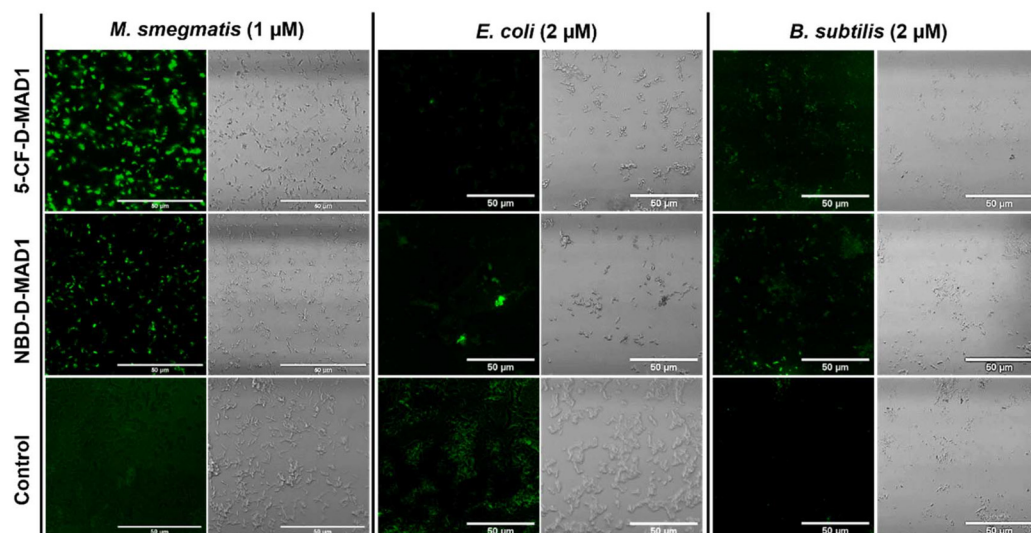


Fig. 2 Specificity of MAD1-based probes for *M. smegmatis* against Gram-negative (*E. coli*) and Gram-positive (*B. subtilis*) bacteria with **5-CF-D-MAD1** and **NBD-D-MAD1**. The bacteria were incubated with the probes for 1 h, washed, and imaged ($\lambda_{\text{ex/em}}$ 480/505 nm). Control = unlabelled cells. Scale bar = 50 μm .

concentration-dependent labelling (Fig. 1A and ESI Fig. S1, S2†). **5-CF-MAD1** showed the strongest labelling, even at 1 μM , not surprising as 5-carboxyfluorescein conjugates are known to have high emissions at physiological pH (Table 1).³⁸ For **5-CF-MAD1** better imaging was achieved using a washing step to reduce the background from the “always-on” probes; however, such background issues were avoided with **NBD-MAD1** and **MeroCy-MAD1** decorated with the environmentally sensitive fluorophores (ESI Fig. S3†). The probes synthesised with D-amino acids showed no pronounced difference to the L-enantiomers (Fig. 1B and ESI Fig. S1, S2†), and the labelling intensity of the MAD1-conjugates remained strong even 24 h after initial labelling (ESI Fig. S4†).

To evaluate the mycobacterial specificity of the probes, the labelling of two common pathogenic Gram-negative and Gram-positive bacteria, *Escherichia coli* and *Bacillus subtilis*, were examined with **5-CF-D-MAD1** and **NBD-D-MAD1** by confocal microscopy (Fig. 2). Neither **5-CF-D-MAD1** nor **NBD-D-MAD1** showed labelling at 2 μM , showing *M. smegmatis* selectivity (Fig. S5†), although at higher concentrations (>5 μM) of the D-enantiomer probes, there was some off-target labelling as previously reported by Medina.²⁷

At low probe concentrations (1 μM), there was no labelling of *Mtb* strain *H37Rv* by **NBD-D-MAD1**, **5-CF-D-MAD1**, or **MeroCy-D-MAD1**; however, both **5-CF-D-MAD1** and **NBD-D-MAD1** (10 μM) showed labelling of *H37Rv* whereas **MeroCy-**

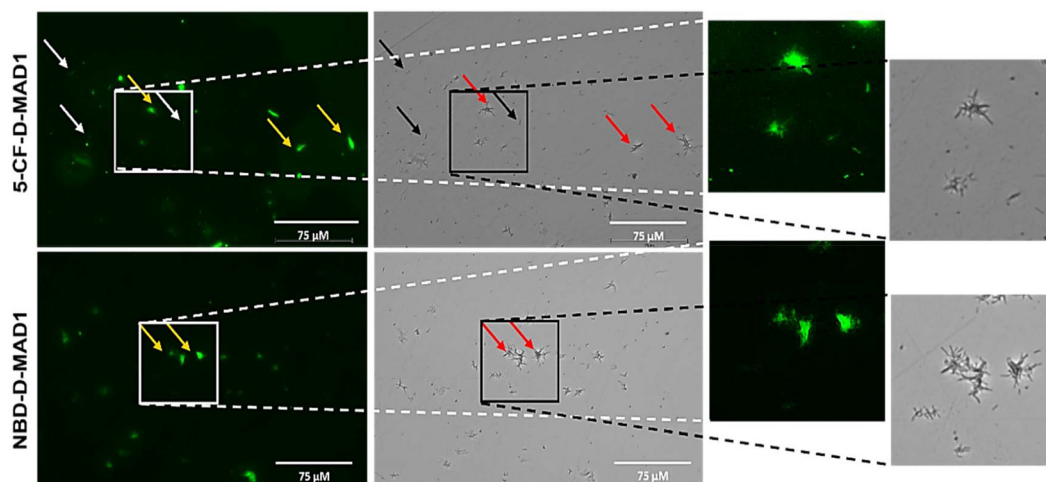


Fig. 3 Fluorescent labelling of the pathogenic *Mtb* strain *H37Rv* by incubation with **5-CF-D-MAD1** and **NBD-D-MAD1** (10 μM) for 1 h, followed by washing with PBS and imaging at $\lambda_{\text{ex/em}}$ 488/505 nm using fluorescence microscopy. **5-CF-D-MAD1** brightly stained both *Mtb* cords and individual bacteria, whereas **NBD-D-MAD1** only stained cord structures. The yellow/red arrows indicate cords and white/black arrows individual bacteria. Regions of special interest have been expanded for clarity (right). Scale bar = 75 μm .



D-MAD1 did not exhibit any significant labelling (here, the D-peptides were used for their better stability in a biological setting). **5-CF-D-MAD1** and **NBD-D-MAD1** were observed to stain *Mtb* cords (end-to-end and side-to-side bacterial attachment structures) (Fig. 3).^{39,40} It should be noted that at 10 μ M of **5-CF-D-MAD1**, there would be non-specific labelling of other bacterial species (Fig. S6†); however, in clinical TB diagnosis sample preparation/decontamination often involves destruction of other microbial species through treatments such as *N*-acetyl L-cysteine (NALC) coupled with 2% NaOH, or tri-sodium phosphate with benzalkonium detergents.⁴¹

Conclusions

To selectively identify and label mycobacteria, the MAD1 peptide was chosen as a targeting moiety. Both L- and D-enantiomers of the peptide were synthesised and decorated with different “green” and “far-red” fluorophores. Two solvato-fluorogenic dyes were used to minimise any interference from background autofluorescence. The labelling efficiency of the MAD1-based probes were investigated on *M. smegmatis*, with all the probes showing robust and stable mycobacterial labelling and concentration-dependent specificity against common pathogenic Gram-negative and Gram-positive bacteria. Notably, **5-CF-D-MAD1** and **NBD-D-MAD1** showed potential for early TB screening by labelling clinically relevant forms of *Mtb*, although labelling was much reduced compared to *M. smegmatis*.

Data availability

The data supporting this article have been included as part of the ESI.†

Conflicts of interest

There are no conflicts to declare.

Acknowledgements

Z. S. A. thanks the Saudi Arabian Ministry of Higher Education and the Chemistry Department in Imam Abdulrahman Bin Faisal University for a PhD scholarship. R. S. thanks The Royal Society, UK and The Science and Engineering Research Board, India for a Newton-Bhabha International Fellowship and European Commission's Horizon 2020 research and innovation program under grant agreement No 825931 (ARREST-TB).

Notes and references

- 1 The World Health Organization, Global Tuberculosis Report 2022.
- 2 T. Ryckman, K. Robsky, L. Cilloni, S. Zawedde-Muyanja, R. Ananthakrishnan, E. A. Kendall, S. Shrestha, S. Turyahabwe, A. Katamba and D. W. Dowdy, *Lancet Infect. Dis.*, 2023, **23**, 59–66.
- 3 The World Health Organization, Global Tuberculosis Report 2021.
- 4 The World Health Organization, Global Tuberculosis Report 2019.
- 5 F. Ziehl, *Dtsch. Med. Wochenschr.*, 1882, **8**, 451–451.
- 6 P. Hagemann, *Münch. Med. Wochenschr.*, 1938, **85**, 1066–1068.
- 7 E. G. Dzodanu, J. Afrifa, D. O. Acheampong and I. Dadzie, *Tuberc. Res. Treat.*, 2019, **2019**, 4091937.
- 8 S. Asmar and M. Drancourt, *Front. Microbiol.*, 2015, **6**, 1184.
- 9 M. R. Rios, G. Garoffolo, G. Rinaldi, A. Megia-Fernandez, S. Ferrari, C. T. Robb, A. G. Rossi, M. Pesce and M. Bradley, *Chem. Commun.*, 2021, **57**, 97–100.
- 10 A. Baibek, M. Üçüncü, E. A. Blackburn, M. Bradley and A. Lilienkampf, *Pept. Sci.*, 2021, **113**, e24167.
- 11 R. Sharma, H. Rajagopalan, M. Klausen, M. V. Jeyalatha, M. Üçüncü, S. Venkateswaran, A. R. Anand and M. Bradley, *Sens. Diagn.*, 2022, **1**, 1014–1020.
- 12 R. S. Valand and A. Sivaiah, *J. Mater. Chem. B*, 2023, **11**, 2614–2630.
- 13 K. E. Beatty, M. Williams, B. L. Carlson, B. M. Swarts, R. M. Warren, P. D. Van Helden and C. R. Bertozzi, *Proc. Natl. Acad. Sci. U. S. A.*, 2013, **110**, 12911–12916.
- 14 W. Chyan and R. T. Raines, *ACS Chem. Biol.*, 2018, **13**, 1810–1823.
- 15 X. Wu, W. Shi, X. Li and H. Ma, *Acc. Chem. Res.*, 2019, **52**, 1892–1904.
- 16 K. M. Backus, H. I. Boshoff, C. S. Barry, O. Boutureira, M. K. Patel, F. D'hooge, S. S. Lee, L. E. Via, K. Tahlan and C. E. Barry III, *Nat. Chem. Biol.*, 2011, **7**, 228–235.
- 17 B. M. Swarts, C. M. Holsclaw, J. C. Jewett, M. Alber, D. M. Fox, M. S. Siegrist, J. A. Leary, R. Kalscheuer and C. R. Bertozzi, *J. Am. Chem. Soc.*, 2012, **134**, 16123–16126.
- 18 F. P. Rodriguez-Rivera, X. Zhou, J. A. Theriot and C. R. Bertozzi, *J. Am. Chem. Soc.*, 2017, **139**, 3488–3495.
- 19 H. L. Hodges, R. A. Brown, J. A. Crooks, D. B. Weibel and L. L. Kiessling, *Proc. Natl. Acad. Sci. U. S. A.*, 2018, **115**, 5271–5276.
- 20 N. J. Holmes, H. W. Kavunja, Y. Yang, B. D. Vannest, C. N. Ramsey, D. M. Gepford, N. Banahene, A. W. Poston, B. F. Piligian and D. R. Ronning, *ACS Omega*, 2019, **4**, 4348–4359.
- 21 T. Dai, J. Xie, Q. Zhu, M. Kamariza, K. Jiang, C. R. Bertozzi and J. Rao, *J. Am. Chem. Soc.*, 2020, **142**, 15259–15264.
- 22 S. S. Nalpe, S. Jana and S. S. Kulkarni, *Org. Lett.*, 2023, **25**, 1717–1721.
- 23 N. Banahene, D. M. Gepford, K. J. Biegas, D. H. Swanson, Y. P. Hsu, B. A. Murphy, Z. E. Taylor, I. Lepori, M. S. Siegrist and A. Obregón-Henao, *Angew. Chem.*, 2023, **135**, e202213563.
- 24 A. Baibek, *Fluorescent probes for microorganisms*, PhD thesis, University of Edinburgh, 2022.
- 25 N. J. Afacan, A. T. Y. Yeung, O. M. Pena and R. E. W. Hancock, *Curr. Pharm. Des.*, 2012, **18**, 807–819.



- 26 E. F. Haney, S. K. Straus and R. E. Hancock, *Front. Chem.*, 2019, **7**, 435645.
- 27 A. W. Simonson, A. S. Mongia, M. R. Aronson, J. N. Alumasa, D. C. Chan, A. Lawanprasert, M. D. Howe, A. Bolotsky, T. K. Mal, C. George, A. Ebrahimi, A. D. Baughn, E. A. Proctor, K. C. Keiler and S. H. Medina, *Nat. Biomed. Eng.*, 2021, **5**, 467–480.
- 28 A. W. Simonson, T. M. Umstead, A. Lawanprasert, B. Klein, S. Almarzooqi, E. S. Halstead and S. H. Medina, *Biomaterials*, 2021, **273**, 120848.
- 29 X. Zhu, Z. Ma, J. Wang, S. Chou and A. Shan, *PLoS One*, 2014, **9**, e114605.
- 30 A. W. Simonson, M. R. Aronson and S. H. Medina, *Molecules*, 2020, **25**, 2751.
- 31 A. Brunet, T. Aslam and M. Bradley, *Bioorg. Med. Chem. Lett.*, 2014, **24**, 3186–3188.
- 32 Y. Bai, Y. Huang, W. Wan, W. Jin, D. Shen, H. Lyu, L. Zeng and Y. Liu, *Chem. Commun.*, 2021, **57**, 13313–13316.
- 33 A. Megia-Fernandez, B. Mills, C. Michels, S. V. Chankeshwara, N. Krstajić, C. Haslett, K. Dhaliwal and M. Bradley, *Org. Biomol. Chem.*, 2018, **16**, 8056–8063.
- 34 M. Rodriguez-Rios, G. Rinaldi, A. Megia-Fernandez, A. Lilienkampf, C. Robb, A. Rossi and M. Bradley, *Chem. Commun.*, 2023, **59**, 11660–11663.
- 35 C. J. MacNevin, D. Gremyachinskiy, C.-W. Hsu, L. Li, M. Rougie, T. T. Davis and K. M. Hahn, *Bioconjugate Chem.*, 2013, **24**, 215–223.
- 36 A. Megia-Fernandez, M. Klausen, B. Mills, G. E. Brown, H. McEwan, N. Finlayson, K. Dhaliwal and M. Bradley, *Chemosensors*, 2021, **9**, 117.
- 37 A. J. Lander, Y. Jin and L. Y. Luk, *ChemBioChem*, 2023, **24**, e202200537.
- 38 U. Anthoni, C. Christophersen, P. H. Nielsen, A. Püschl and K. Schaumburg, *Struct. Chem.*, 1995, **6**, 161–165.
- 39 T. R. Lerner, C. J. Queval, R. P. Lai, M. R. Russell, A. Fearn, D. J. Greenwood, L. Collinson, R. J. Wilkinson and M. G. Gutierrez, *JCI Insight*, 2020, **5**, e136937.
- 40 A. G. V. Coelho, L. A. Zamarioli, C. M. P. V. Reis and B. F. de Lima Duca, *J. Bras. Pneumol.*, 2007, **33**, 707–711.
- 41 M. Chatterjee, S. Bhattacharya, K. Karak and S. G. Dastidar, *Indian J. Med. Res.*, 2013, **138**, 541–548.

